



Universiteit  
Leiden  
The Netherlands

## **Mapping Massive Migrations: Spatiotemporal spread of Corded Ware in the Czech Republic, Poland and the Eastern Baltics during the 3rd Millennium BCE**

Grave, Alissa

### **Citation**

Grave, A. (2023). *Mapping Massive Migrations: Spatiotemporal spread of Corded Ware in the Czech Republic, Poland and the Eastern Baltics during the 3rd Millennium BCE*.

Version: Not Applicable (or Unknown)

License: [License to inclusion and publication of a Bachelor or Master Thesis, 2023](#)

Downloaded from: <https://hdl.handle.net/1887/3640819>

**Note:** To cite this publication please use the final published version (if applicable).

# Mapping Massive Migrations:

Spatiotemporal spread of Corded Ware in the Czech Republic, Poland and the Eastern Baltics during the 3<sup>rd</sup> Millennium BCE

Alissa Grave



Cover figure:

<https://www.mapchart.net/europe.html>

Rudnicki, M., & Włodarczak, P. (2007). Graves of the Corded Ware culture at the multicultural site 6 in Pełczyska, district of Pińczów. *Sprawozdania Archeologiczn*, 59.

# **Mapping Massive Migrations:**

**Spatiotemporal spread of Corded Ware in the Czech Republic, Poland and the Eastern Baltics during the 3<sup>rd</sup> Millennium BCE**

Alissa Grave S2970813

Thesis BA3 1083VBTHEY

Supervisor: Dr. Q.P.J. Bourgeois

University of Leiden, Faculty of Archaeology

Leiden, 15 June 2023 – final version

## **Acknowledgements**

I would like to thank Dr. Bourgeois as well as PhD candidate Florian Helmecke not only for the exciting idea that inspired this thesis, but also for all of their help, feedback and encouragement along the way. I am grateful to be ending my bachelor degree journey under their supervision.

# Table of Contents

1. Introduction	
1.1 Research problem .....	6
1.2 Research questions .....	7
1.3 Thesis outline .....	7
2. Background	
2.1 Research area.....	8
2.2 What is Corded Ware?.....	9
2.3 Burial practices.....	10
3. Methods	
3.1 Selection of burial sites	
3.1.1 Direct samples.....	11
3.1.2 Standard deviation.....	11
3.1.3 Freshwater reservoir effect .....	12
3.1.4 Corded Ware elements .....	12
3.1.5 Overall quality.....	13
3.2 Radiocarbon date calibration.....	13
3.3 Spatiotemporal methods and QGIS	
3.3.1 On spatiotemporal mapping.....	15
3.3.2 Temporal Controller in QGIS.....	16
3.3.3 IDW Interpolation in QGIS .....	18
4. Results.....	21
5. Discussion	
5.1 Temporal controller maps Interpretation.....	24
5.2 IDW interpolation maps interpretation.....	24
5.3 Interpretation side by side .....	25
5.4 Comparison of models.....	25
5.5. Limitation .....	27
6. Conclusion	

6.1 Findings .....	29
6.2 Future directions.....	30
Bibliography .....	32
Abstract.....	37
List of figures.....	38
Appendix A.....	39

# 1. Introduction

Already in the 4<sup>th</sup> millennium BC, a movement of genetic material took place from the Pontic-Caspian steppes westward into Europe, as confirmed by ancient DNA evidence (Haak et al., 2015, p. 207; Allentoft et al., 2015, p. 168; Mittnik et al., 2018, p. 2). This steppe ancestry is commonly linked to the archaeological unit known as the Yamnaya, whose kurgan burials and material culture too show a pattern of expansion from the steppes in the late 4<sup>th</sup> millennium BC (Heyd, 2021, p. 385-386). It was long assumed that the Yamnaya gave rise to Corded Ware in eastern and central Europe, in part because Corded Ware burial customs can be viewed as being inspired by the Yamnaya (Heyd, 2021, p. 387). It is easy to assume that the people carrying steppe DNA brought elements of their culture with them as they moved out of the steppe, which were then adopted or adapted within Europe to form a new cultural unit. However, to what extent the appearance of steppe ancestry relates to the emergence of Corded Ware is still up for debate. For example, recent research into Early Corded Ware individuals from Bohemia showed a dynamic genetic history with highly variable amounts of DNA from the steppe region, ranging from no steppe ancestry to significant proportions of steppe ancestry (Papac et al., 2021, p. 9). How the subsequent movement of the Corded Ware material culture across the Europe continent took place is similarly debatable, considering the various theoretical models in existence (see e.g. Nordqvist & Heyd, 2020).

## 1.1 Research problem

In light of the above discussion, investigating the real world spatiotemporal spread of Corded Ware has significant potential to contribute. It could inform about core areas where Corded Ware culture first appeared, how it moved across the continent and what that means for our understanding of the culture in a wider context. However, as of yet there have been little to no sophisticated attempts at analyzing what the collective quantitative data says about the spatiotemporal spread of Corded Ware. The aim of this thesis is to contribute to this debate through a well refined attempt at visualizing available data using open-source GIS software. The data used here was provided through the research project “The Talking Dead”, overseen by Dr. Bourgeois (Nederlandse Organisatie voor Wetenschappelijk Onderzoek, n.d.). This data consists of large data sheets containing information about individual Corded Ware burials, including their location coordinates, raw radiocarbon dates, grave finds, et cetera. For the scope of this thesis, the research area will be restricted to the data from the Czech Republic, Poland, and the Eastern Baltic countries of Estonia, Latvia and Lithuania.



## 1.2 Research questions

The main research question of this thesis is as follows:

What was the spatiotemporal spread of Corded Ware burial practices in the Czech Republic, Poland, and the Eastern Baltics during the 3<sup>rd</sup> millennium BC?

To answer this question, the following sub-questions are posed:

1. What criteria should be used to select reliable radiocarbon-dated Corded Ware burial sites in the research area?
2. What spatiotemporal GIS method is most suitable for mapping the selected burial sites in QGIS?
3. According to the spatiotemporal maps, where can we identify the oldest core area (or areas) where Corded Ware culture originated from within the research area?
4. According to the spatiotemporal maps, what is the direction of movement out of this core area (or areas)?
5. How do the patterns that emerge from the spatiotemporal GIS maps compare to existing models for the movement of Corded Ware culture during the 3<sup>rd</sup> millennium BC?

## 1.3 Thesis outline

Starting off in chapter 2, I will provide a general background on the research area, including an overview of the characteristics of Corded Ware culture as an archaeological unit in general, and more specifically the burial practices associated with the culture. In chapter 3 on methods, I will give an in depth description of the criteria that were used to select the final set of Corded Ware burials from a large dataset. Additionally, I will delve into the process of calibrating the dates and a brief introduction on the application of spatiotemporal GIS. Then, I will demonstrate how the data was used and visualized in QGIS in two distinct ways. The results of this are presented in chapter 4. Chapter 5 focuses on a comprehensive examination of the results. The results will be interpreted and compared to existing theories and models. Last but not least, in the concluding chapter 6, the findings of this research are summarized, and suggestions for future research endeavors are made.

## 2. Background

In order to contextualize the research in this thesis, it is necessary to provide some additional background information. The research area and why it was chosen will be covered first, followed by some general background on the Corded Ware archaeological unit, as well as on Corded Ware burial practices specifically.

### 2.1 Research Area

Corded Ware has a very wide distribution covering many countries in eastern and central Europe, but also stretches all the way to the Netherlands in the west, and Finland in the north (Nordqvist & Heyd, 2020, p. 66). A subset of countries that are known to have Corded Ware sites were chosen as the research area, namely the Czech Republic, Poland, and the Eastern Baltic countries of Estonia, Lithuania and Latvia (see figure 1). The Russian province of Kaliningrad, situated between Lithuania and Poland, was not included as there is currently no data available on Corded Ware from this region.

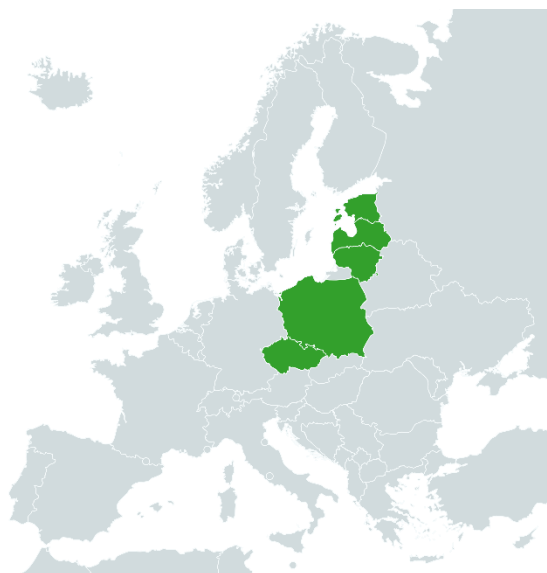


*Figure 1* The research area indicated in green on a map of Europe. The countries are adjacent to one another (<https://www.mapchart.net/europe.html>).

The chosen countries together represent a significant portion of known Corded Ware burial sites, and provide sufficient data to work with in this thesis. Considering the ongoing debate on steppe ancestry and its relevance for the appearance and spread of Corded Ware, these are also the countries where a decent amount data for recent ancient DNA studies came from (e.g. Allentoft et al., 2015, p. 168; Mittnik et al., 2018, p.3) Additionally, the research area can be seen as a corridor for the dispersal of steppe ancestry and/or Corded Ware cultural elements, including burial practices, to the extremities of Corded Ware distribution. Movement patterns in this area are therefore particularly interesting.

## 2.2 What is Corded Ware?

Corded Ware, like many archaeologically defined units, is characterized by a number of different individual elements that we can recognize in material culture. Objects from the so-called “A-Horizon”, including a specific type of beaker, amphora, and battle axe were once thought to be the quintessential early Corded Ware elements (Dobeš et al., 2021, p. 487), displaying a tendency for new elements to be taken as typical. Corded Ware did indeed come with several new cultural elements. Prior to the appearance of Corded Ware, individual inhumations were relatively rare (Champion et al., 2009, p. 171). Gender differentiation in burials is also something the potential Corded Ware predecessor, the Yamnaya, did not do (Nordqvist & Heyd, 2020, p. 85, see chapter 2.3). It is however very unlikely that all Corded Ware elements shared the same origin (Furholt, 2014, 70-71), and A-type objects have been found throughout the entire Corded Ware sequence (Vander Linden, 2007, p. 182). Corded Ware material also occurs alongside other archaeological cultures in many regions (Nordqvist & Heyd, 2020, p. 72). All of this begs the question; what really defines Corded Ware?

The classification by archaeologists of Corded Ware as closed-off unit gives the impression of internal homogeneity, which in turn can seep into interpretations of various aspects of Corded Ware culture, including population movement. Classifications are not a perfect reflection of reality, but categorization of some kind is nevertheless necessary in order to make sense of our surroundings. It is an essential backbone and tool to any investigation (Furholt, 2003, p. 13). Perhaps a more polythetic definition of what can be considered Corded Ware is useful, like the one described by Martin Furholt (2020). Not every element associated with Corded Ware needs to be present for a site to be considered Corded Ware. Shared elements within the unit are also not restricted to the unit, but can indeed exist outside of it (Furholt, 2020, p. 3). This definition is much more flexible than a traditional classification. With a more polythetic approach in mind, Furholt also formulated the concept of the ‘Late Neolithic and Early Bronze Age Single Grave Burial Ritual Complex’ or SGBR, which is a wider concept based on a few main element, while connected to variable sets of material culture and social groups (Furholt, 2019, p. 3-4). The author also suggests a much more secure tie between SGBR and steppe ancestry than between Corded Ware and steppe ancestry (Furholt, 2019, p. 6).

While a concept like SGBR could be fascinating regarding the migration debate, the data available for use in this investigation specifically represents the Corded Ware label only. However, a somewhat polythetic approach will be used when making a selection of burials to use within the main method (see chapter 3.1.4.)

## 2.3 Burial practices and grave goods

This thesis exclusively presents and uses data from burial sites. While Corded Ware settlement sites do exist, the amount of data varies widely depending on the region. In the Czech Republic, very few settlements are known (Furholt, 2020, p. 11). Meanwhile in the Eastern Baltics, Corded Ware settlement sites are quite numerous (Nordqvist & Heyd, 2020, p. 72), with relatively few and smaller burial grounds (Löugas et al., 2007, p. 23). The reason for this might be related to differences in lifestyles with varying degrees of mobility. Settlement sites also tend to follow regionally or locally defined standards while burial rites and pottery styles tend to be transregional (Furholt, 2020, p. 7), so similar or identical funerary practices can be expected throughout the research area. For the above reasons, Corded Ware burials can be easier to recognize and are a more consistent and source of data. Hence, the focus here is on burials.

Individuals associated with Corded Ware are buried in a semi-flexed or crouched position, and are furthermore oriented differently based on the individual's gender. In Corded Ware, men were buried on their right side, facing south with their heads to the west, while women were buried on their left side, facing south with their heads to the east (Bourgeois & Kroon, 2017, p. 1). Regarding grave goods, it may come as no surprise that ceramics are the biggest find category in Corded Ware burials (Nordqvist & Heyd, 2020, p. 72). Beakers and amphorae, often with cord impressions, are typical pottery forms (Furholt, 2014, p. 70). Other grave goods include stone or flint battle axes, flint blades, flint arrowheads as well as pendants, ornaments, beads and pins out of various materials including Baltic amber, shell, animal bone or teeth and antler. Differences in grave goods between men and women have also been observed. Women tended to receive more ornamental objects (Vander Linden, 2007, p. 183). Male individuals, on the other hand, are more often associated with specific weapons, possibly related to the warrior role (Furholt, 2020, p. 6). Male burials are also more similar across large areas than women's burials, which could further indicate a male-focused society (Bourgeois & Kroon, 2017, pp. 13–14).

### **3. Methods**

The main method used to answer the research questions involves geographic information systems (GIS). However, in order to make maps that live up to a certain level of quality and scientific accuracy, a few other steps were required in advance. Only good quality input produces good quality output. Therefore, all the data was carefully examined and selected based on a few criteria that are defined in order to answer the first research question. The data was then reformatted and calibrated for use in GIS software. Two different methods within GIS are employed to allow for comparisons and an answer to the second research question.

#### **3.1 Selection of burial sites**

In order to safeguard the quality of the final maps, it is necessary to evaluate each burial site and its associated radiocarbon date critically. The selection process of dated burial sites to be included in the map followed the criteria below.

##### **3.1.1 Direct sampling**

When taking a sample for the radiocarbon dating of a burial, the most reliable samples come from within the grave pit. These samples can be referred to as direct samples. The most straightforward direct samples in the case of burials are those from human skeletal remains. However, direct charcoal samples or samples from animal materials that were included as grave gifts can also be direct samples. It is important to note that charcoal samples might suffer from the old wood effect; if wood was cut down many years before it was burned, a  $^{14}\text{C}$  sample will suggest an older date (Furholt, 2003, p. 20). In any case though, samples from outside and around the grave pit cannot guarantee a direct association between the burial and the radiocarbon date, so they are less likely to provide an accurate date for the inhumation. Thus, dates that were derived from indirect samples are excluded from the dataset.

##### **3.1.2 Standard deviation**

Radiocarbon dates with a high standard deviation, often characteristic of dates that were obtained many years ago, are less precise and thus of a lower quality (Włodarczak, 2009, p. 739). Defining a standard deviation threshold can help to filter out these dates. A lower threshold reduces the likelihood of including outliers that could skew the overall analysis. However, it is important to still hold on to enough data so that patterns can be identified when all the data is presented on a spatiotemporal map. For this thesis, a standard deviation threshold of 60 years was chosen. This standard deviation threshold seems to provide a good balance, as it leaves a big enough sample size

to work with while still adhering to a certain level of temporal precision. Any data with a standard deviation higher than 60 will therefore be excluded from the dataset.

### 3.1.3 Freshwater reservoir effect

One problem associated with radiocarbon dating as a result of natural conditions, is the freshwater reservoir effect, or FRE (Włodarczak, 2009, p. 741). FRE can occur at any archaeological sites close to aquatic environments, including Corded Ware sites.  $^{14}\text{C}$  concentrations in aquatic environments are different from those in the atmosphere. Lower  $^{14}\text{C}$  activity in these environments can be transferred through food chains; organisms, including humans, can start to reflect the different  $^{14}\text{C}$  concentration through their diet (Pospieszny, 2015, p. 264). When a human individual has a diet that is heavily reliant on food from an aquatic environment, like fish or shellfish, it is likely that a radiocarbon dating of their archaeological remains is affected by FRE. This means that measurements will indicate an inaccurate older date, which can puzzle archaeologists. This was the case at the Ząbnie site in Poland, which is situated on an island in a lake. Previously obtained radiocarbon dates were surprisingly old and did not fit the expected ages of the graves present at the site (Pospieszny, 2015, p. 268). One way to deal with the FRE, is by dating other materials from the same context that are unlikely to be affected, like the T-shaped antler plate that was found in grave 398 at Ząbnie (Pospieszny, 2015, p. 274). Bone, teeth or antlers from terrestrial animals that do not rely on aquatic foods could provide a sample that gives a more accurate dating. Aquatic foods were extensively exploited at the site of Zvejnieki in northern Latvia too (Meadows et al., 2016, p. 1), meaning many of the graves at the site might be affected by FRE. However, stable isotope data suggests a terrestrial date for at least one grave on the site, number 137 (Meadows et al., 2014, p. 830). For the above reasons, both Ząbnie398 and Zvejnieki137 were still included in the final dataset.

### 3.1.4 Corded Ware elements

Following the polythetic approach described in chapter 2.2., burials were selected where several Corded Ware cultural elements are present in the same context, but no single element was absolutely essential to qualify a sample for inclusion in the final selection. For example, the individual that provided the  $\text{C}^{14}$  sample might have been found in typical Corded Ware fashion crouched on their side according to their gender, but there are no grave goods present that link the grave to the Corded Ware culture. Dated burials without grave goods were only accepted if Corded Ware artefacts were discovered in a secure context at the same site, which was the case for grave 241 at Plinkaišalis in Lithuania (Antanaitis-Jacobs et al., 2009, p. 18) and grave 46a at Magnice in Poland (Baron et al., 2019, p. 172). These two graves were therefore included.

### 3.1.5 Overall quality

There are a number of other reasons why a dated sample might be considered of lower quality. The context of the sample might be ambiguous or uncertain, because of either modern or ancient disturbances (Taylor & Bar-Yosef, 2016, p. 134); some samples were excluded because the grave in question was damaged by modern land use or because there was evidence of grave reopening in the past. Contamination of the sample can also cause an unreliable younger or older dating (Taylor & Bar-Yosef, 2016, p. 134), and can happen in a number of ways. Furthermore, there might simply be no or insufficient information available in published works about the quality of a sample (Pospieszny, 2015, p. 268), which can make a sample unreliable. Beyond the sampling stage, different laboratories can also give different results at different times, although modern technique improvements have made recent datings more consistent than older ones (Furholt, 2003, p. 18). The original dataset has already taken some of these reasons into account, or made notes of such problems.

Lastly, some of the burial sites do not have a precise known coordinate in the original dataset. For the research presented here, this level of imprecision is not an issue, and it is not an indicator of a poor quality radiocarbon date. The scale of the maps will be large, as they will cover multiple countries, and no precise measurements of distance will be made. A rough location is therefore sufficient. So, if a sample fits all other criteria, the coordinates can simply be estimated using the toponym in Google Maps (<https://www.google.com/maps>) and the sample can still be included.

After filtering the original dataset based on the above criteria, 50 dated samples remained. Some of these are from different burials at the same burial site, meaning the total number of locations is slightly lower than 50. The final dataset that was used can be found in Appendix A.

## 3.2 Radiocarbon date calibration

The amount of  $^{14}\text{C}$  in the atmosphere has varied throughout time due to a number of factors, including sun spot activity, changes in ocean and biosphere activity, and more recently due to the use of fossil fuels and nuclear weapons testing (Scott & Reimer, 2009, p. 283). Organisms like plants and animals reflect these fluctuating atmospheric  $^{14}\text{C}$  concentrations during their life, but it is when an organism dies and metabolic processes stop that the  $^{14}\text{C}$  in their remains will start to decay (Taylor & Bar-Yosef, 2016, p. 22). This is why it is important for archaeologists to consider the amount of  $^{14}\text{C}$  that would have been present in any sample before the process of decay started in order to get an accurate dating. That is where radiocarbon calibration comes in. Radiocarbon dating

results need to be calibrated against either <sup>14</sup>C measurements from material with a known calendar age or against independently dated material (Reimer et al., 2020, p. 726). The available data for this thesis consists of uncalibrated radiocarbon dates. Thus, in order to prepare these raw dates for use in a GIS, it is necessary to calibrate them and turn them into calendar years.

An easy and very accessible way to calibrate raw radiocarbon dates is using OxCal Online, a free calibration platform available in any browser (<https://c14.arch.ox.ac.uk/oxcal/OxCal.html>). OxCal comes with several standard calibration curves. The curve used to calibrate our dates is the IntCal20 calibration curve, which is the most recent IntCal curve. It is part of a collection of three calibration curves; IntCal20 is specifically intended for Northern Hemisphere atmospheric samples (Reimer et al., 2020, p. 727). It is based on a combination of data from various materials, but the primary source of data is tree rings. Dendrochronological data extends to 13.910 cal BP, and this part of the curve is therefore fully atmospheric, but the older part also incorporates data from marine sediments and stalagmites, among others (Reimer et al., 2020, p. 743). IntCal20 was used in OxCal to generate a probability distribution of likely calibrated ages for each of the 50 selected samples by entering the raw BP dates along with the standard deviations. An example of a calibration plot can be found in figure 2.

The resulting calibrated ages are typically given as sigma ranges. The 1 sigma range has a 68.2% probability, the 2 sigma range has 95.4% probability and the 3 sigma range has a 99.7% probability. However, the two different QGIS methods used in this thesis required different data from the calibrated dates (see also chapter 3.3.2 and 3.3.3). For the method involving the temporal controller, just one specific date per burial was needed to be shown on the maps. For this purpose it was decided to use the mean date ( $\mu$ ) of each distribution. The method involving interpolation required a lot of precise probability data from each distribution curve. This will be elaborated on more in chapter 3.3.3.

One thing to note about calibration curves is that the amount of certainty they offer is not consistent. A calibration curve is not perfectly linear, and includes plateaus. These plateaus represent times during which atmospheric <sup>14</sup>C concentrations barely changed. The ability to reach a high temporal resolution during these periods is inherently reduced, if dating is based solely on the radiocarbon method (Taylor & Bar-Yosef, 2016, p. 156). There are two notable plateaus during the 3<sup>rd</sup> millennium BC, namely between 2880 and 2580 BC and between 2470 and 2200 BC the first of which so happens to coincide with Corded Ware settlement in most regions ( Nordqvist & Heyd, 2020, p. 69). This is an issue inherent to the <sup>14</sup>C method, and cannot be omitted without the incorporation of other dating methods that go beyond the scope of this thesis.



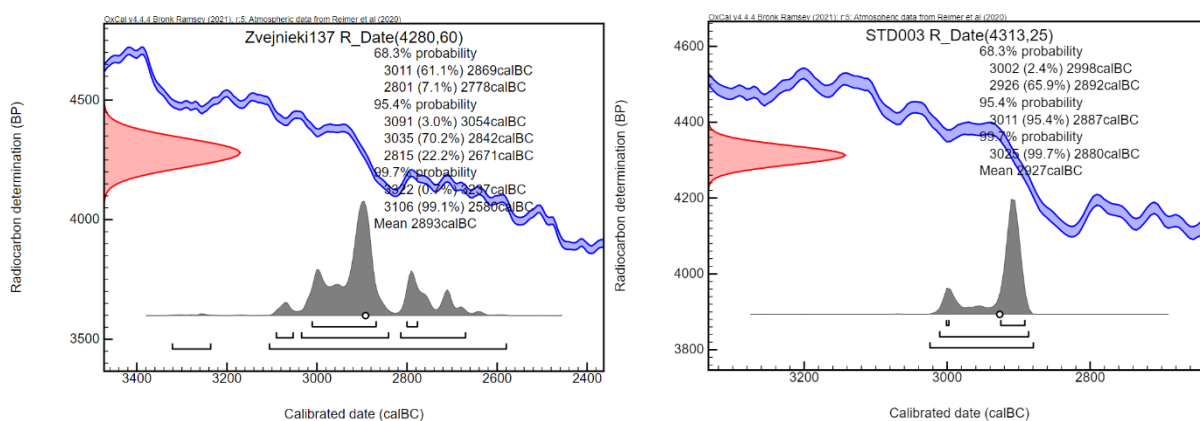


Figure 2 Two examples of different looking calibration plots in OxCal v4.4.4. Grave 137 at the Zvejnieki site in Latvia (Zvejnieki137) has a mean ( $\mu$ ) calibrated age of 2893 BC, and grave 67/87 at the Stadice site in the Czech Republic (STD003) has a mean ( $\mu$ ) calibrated age of 2927 BC (<https://c14.arch.ox.ac.uk/oxcal/OxCal.html#>).

### 3.3 Spatiotemporal methods and QGIS

The GIS software used in our research is the free open-source software QGIS (*Discover QGIS*, n.d.) and more specifically QGIS version 3.30.1, which is the most recent version at the time of writing this thesis. QGIS is ran by volunteers, and there is a large community around it making it a very accessible and user-friendly option. This thesis will explore two different ways of visualizing spatiotemporal data in QGIS.

#### 3.3.1 On Spatiotemporal Mapping

Visualizing spatiotemporal processes provides a way to present and analyze data that varies not only across geographical space, but also across different points in time. Data used for this purpose is typically time series data; data that is geographically referenced and recorded at regular intervals over a specific period of time. There are many strategies for portraying such data. Already in 1990, Monmonier described various methods, which he categorizes as single-static, multiple-static, single dynamic or multiple dynamic (Monmonier, 1990, p. 44). One simple way to make a static map is by implementing flow-linkage diagrams with directional symbols like arrows. A multiple-static way would be a static print layer showing snapshots of specific time intervals side by side; juxtaposing the images allows the reader to easily compare spatial patterns. Dynamic methods can add an extra dimension through animation techniques. Within archaeology, the use of spatiotemporal maps has various applications in the study of population movements and dynamics, including recent research

in regards to prehistoric Europe (see for example Crema et al., 2017; Racimo et al., 2020). As advances are made in GIS and GIS software, the application of spatiotemporal GIS in archaeology could prove to become increasingly powerful.

### 3.3.2 Temporal Controller in QGIS

The first method used within QGIS involved the temporal controller panel. The temporal controller is one of perhaps the two most evident ways to manage time in QGIS; either using the temporal controller panel or the free to download TimeManager plugin (*TimeManager — QGIS Python Plugins Repository*, n.d.). The temporal controller has a lot of inbuilt functionalities based on the TimeManager plugin, but they are not identical. The plugin, once added to your QGIS project, has an Archaeology Mode that allows the use of time data in years only, instead of the yyyy-mm-dd format that the temporal controller requires. Dates in a BC/AD format are also accepted in Archaeology Mode. Meanwhile, neither the BC/AD format nor negative dates to represent BC dates are accepted in the temporal controller. Unfortunately, at the time of writing this thesis, the TimeManager plugin does not work with the newest versions of QGIS. One of the creators of the TimeManager plugin, Anita Graser, personally declared the end of the TimeManager on her blog (Graser, 2020). The plugin has mostly been replaced by the temporal controller panel over time. Old versions of QGIS are still available for download on the internet (*Download QGIS*, n.d.), so the plugin could still be used. However, but for the purpose of this research, the decision was made to favor the use of the latest QGIS software available. Therefore, the temporal controller became the main tool for this method.

In order to work around the restrictions of the temporal controller panel, the negative BC dates needed to be turned into positive numbers, while still maintaining the same order and the same time intervals between each date. To achieve this, an offset of 5000 was used for every date. For example, a calibrated mean ( $\mu$ ) BC date of -2671 BC (burial ID Sope2) is equal to 2329, because  $-2671 + 5000 = 2329$ . Any offset would work as long as all the resulting numbers are positive ( $>0$ ) and smaller than 9999. Anything over 9999 would also not be accepted considering the yyyy-mm-dd format. An offset of 5000 was simply chosen because it is a rounded number that results in numbers that fit these criteria. Additionally, to work with the yyyy-mm-dd format all the offset dates were set to January 1<sup>st</sup>. That makes 2329-01-01 the new date for the Sope2 burial.

All the data used in this method was copied from the original data sheets into a single Excel sheet, with two added columns for the calibrated mean ( $\mu$ ) dates and the reformatted dates (see also Appendix A). This sheet was then saved as a CSV UTF-8 (comma delimited) file. Such a comma separated values (.csv) file can easily be added to QGIS as a Delimited Text vector layer on top of any base map layers. The attribute table of a CSV file cannot be edited once added to QGIS, unless a

plugin like the GeoCSV plugin is used (*Editable GeoCSV — QGIS Python Plugins Repository*, n.d.), so checking the data for mistakes before adding it to QGIS is advised.

The coordinate reference system (CRS) used for the QGIS project is WGS 84 / Pseudo-Mercator EPSG:3857, a widely used CRS that is compatible with various web applications and web mapping services including Google Maps and OpenStreetMap (*EPSG:3857*, n.d.). The Pseudo-Mercator system preserves direction and shape but distorts area and distance and is therefore not ideal for precise measurements, especially far away from the equator. In this case, precise measurements do not matter as the focus is on identifying very general trends. The CRS for the vector layer with coordinate points is EPSG:4326, which is a commonly used CRS that supports coordinates in latitude and longitude (*EPSG:4326*, n.d.). All our coordinates are in latitude and longitude coordinates in decimal degrees, so our data is suitable for this CRS. Typically, the CRS of all layers in a QGIS project should be consistent. However, considering how this method requires no further spatial analysis the EPSG:4326 CRS can still be used for the vector point layer, while EPSG:3857 is set as the project CRS. This will also create in a more aesthetic appearance of the map compared to a project set in EPSG:4326, which would result in a somewhat flattened map (see chapter 3.3.3). QGIS will automatically reproject vector layers to match the project CRS.

The base map used in this project primarily consists of a basic colored DEM (Digital Elevation Model) with added hill shading, taken from Terrestris, an open source provider of maps and spatial information (Terrestris, 2019). The map was added as a layer through web map services (WMS), using the URL available on Terrestris' website. On top of this layer, an overlay layer with national land borders was also included, taken from the Natural Earth public domain map dataset (Natural Earth, n.d.). Although these national borders are not directly relevant for our research, they simply serve as references or visual landmarks for the reader to give them a better spatial orientation.

The symbology of the dots used to mark the location of each site in our vector layer was selected to have a high contrast color against the DEM background. The opacity of the dots was adjusted to 50%. This allows for overlaps among the dots to be visible, as multiple 50% opacity dots layered on top of each other will create a higher color opacity. There are several instances of multiple burials from the same archaeological site or from sites located very close to each other in our dataset, meaning their locations will overlap while one burial might be of a much different age than the other. The adjusted opacity will significantly improve the visibility of these instances on the maps.

Once all the data is added to our project and, the vector layer with our data needs to be made time-aware by turning on dynamic temporal control in the layer's properties. What we have created now is essentially a time aware vector layer. The temporal controller can now animate when and where

our data shows up on the map, and the resulting time series data can be analyzed. Snapshots of the animation presented side-by-side can similarly be used to observe change in a static format. Covering 50 years in each snapshot seemed to be the minimum needed to see at least some change in the majority of the snapshots. This resulted in a time series of 15 maps.

### 3.3.3 IDW Interpolation in QGIS

The second method used in QGIS was chosen to be more spatial analysis focused than the first one. After calibrating all the dates in OxCal, it is possible to run the calibration curves and then export a data report. In this data report, there is a column with probability values for the age of every sample. As shown in figure 3, it lists potential ages with an interval of 5 years next to a column that says how likely it is that the relevant sample is that age according to the calibration.

index	op	name	z	type	value	probability
1	R_Date	Smrokow1		likelihood	-2879.5	0
1	R_Date	Smrokow1		likelihood	-2874.5	0
1	R_Date	Smrokow1		likelihood	-2869.5	9.368e-9
1	R_Date	Smrokow1		likelihood	-2864.5	1.8737e-8
1	R_Date	Smrokow1		likelihood	-2859.5	4.684e-8
1	R_Date	Smrokow1		likelihood	-2854.5	1.3116e-7
1	R_Date	Smrokow1		likelihood	-2849.5	3.185e-7
1	R_Date	Smrokow1		likelihood	-2844.5	7.12e-7
1	R_Date	Smrokow1		likelihood	-2839.5	0.0000017332
1	R_Date	Smrokow1		likelihood	-2834.5	0.000003682
1	R_Date	Smrokow1		likelihood	-2829.5	0.000006333
1	R_Date	Smrokow1		likelihood	-2824.5	0.000007832
1	R_Date	Smrokow1		likelihood	-2819.5	0.000005977
1	R_Date	Smrokow1		likelihood	-2814.5	0.0000029604
1	R_Date	Smrokow1		likelihood	-2809.5	5.621e-7
1	R_Date	Smrokow1		likelihood	-2804.5	7.495e-8
1	R_Date	Smrokow1		likelihood	-2799.5	9.368e-9
1	R_Date	Smrokow1		likelihood	-2794.5	0
1	R_Date	Smrokow1		likelihood	-2789.5	0
1	R_Date	Smrokow1		likelihood	-2784.5	0
1	R_Date	Smrokow1		likelihood	-2779.5	0
1	R_Date	Smrokow1		likelihood	-2774.5	1.8737e-8
1	R_Date	Smrokow1		likelihood	-2769.5	1.8737e-8
1	R_Date	Smrokow1		likelihood	-2764.5	2.8105e-8
1	R_Date	Smrokow1		likelihood	-2759.5	2.8105e-8
1	R_Date	Smrokow1		likelihood	-2754.5	4.684e-8

Figure 3 A snippet of the data report exported by OxCal containing detailed probability data. This shows only the probability of the years -2879.5 to -2754 of grave 1 at the Smrokow site in Poland (<https://c14.arch.ox.ac.uk/oxcal/OxCal.html#>).

One way to use this probability data, is by means of interpolation. There are a variety of interpolation techniques and tools available in QGIS, including TIN (triangulated irregular network), heatmap (kernel density estimation) and IDW (inverse distance weighting) interpolation. For this method, IDW interpolation was chosen; an interpolation technique that estimates values at unknown locations based on nearby known values within a certain cut-off distance (Ikechukwu et al., 2017, p. 357). It is a relatively simple and very widely available method in GIS software, including QGIS (Mitas & Mitasova, 2005, p. 482).

To make the data from the data report usable for interpolation in QGIS, it was first copied into a new Excel sheet, and the years were rounded up to whole numbers for use in interpolation tools. The

coordinates for every site were selected from the final data sheet that was used for the temporal controller method and copied into this new Excel sheet as well. Then, the new sheet needed to be filtered based on one particular potential age at a time. For example, when filtered to only look at sites that had a probability value for the year 3000 BC, 11 of the 50 sites come up, each with a probability value. It is these filtered results that need to be added as vector point layers in QGIS for interpolation. Furthermore, to include the temporal aspect, it was necessary to filter for not just one year, but many years. The time range covered by the probability data is roughly between 3300 BC and 2200 BC. A time interval of 50 years was chosen for the maps again for consistency, meaning that the total number of maps in this case is 25. This also meant that the Excel sheet needed to be filtered and exported to .csv files 25 times. This process was sped up using some Microsoft Visual Basic Analysis (VBA) code that automatically exports the filtered Excel sheet as a .csv to a specified location.

After all 25 .csv files were exported, they were added to QGIS as Delimited Text vector layers. Then, after selecting the IDW interpolation tool from the processing toolbox, the right parameters need to be chosen. The right vector layer needs to be selected, and the interpolation attribute needs to be set to the column containing the probability data. The distance coefficient is set to 2.0 by default, but after some comparison between different coefficients, this was increased to 2.5 considering that the distance between sites can at times be quite significant. The extent of the rendered raster was set to cover the entire research area, and remained consistent for every interpolation. The band rendering was set to singleband pseudocolor, and a color ramp ranging from green to red was chosen, where green stands for a higher probability. This is meant to make the map easier to interpret. This whole process is repeated 25 times, resulting in 25 interpolation raster layers for 25 different points in time.

The project CRS for this method was EPSG:4326 instead of EPSG:3857 (*EPSG:4326*, n.d.). This is because QGIS does not render interpolation raster layers correctly when the project CRS does not match the CRS of the vector layer that was used to make the interpolation raster layer. Like mentioned previously, the CRS of the vector layer needs to be EPSG:4326 because that CRS is compatible with latitude and longitude coordinates, unlike EPSG:3857. The simple solution is to keep the project CRS as EPSG:4326, despite the somewhat flattened appearance this CRS of the final maps.

Since the surface of each map will be covered by the interpolation raster, there is no need for a base map like the DEM that was used when working with the temporal controller. However, the layer containing land borders was important to be included on top of the interpolation raster layers

(Natural Earth, n.d.), to add spatial orientation. The land border layer was automatically reprojected to fit the project CRS.

The interpolation raster layers come in a rectangular shape, and inevitably includes the area that represent the Baltic Sea. The Baltic Sea is not relevant for this research. Removing this area from the raster layers will also make the coastline recognizable on the maps, since coastlines are not included in the land borders layer. To do this, a polygon mask layer was made by manually tracing the coastline of the Baltic Sea with a polygon tool and closing it to cover the entire land surface area that is needed for the maps. This polygon shape was then used to clip each of the 25 interpolation raster layers.

With this additional time series data of 25 maps, it is now possible to analyze and compare the two methods in the following chapters 4 and 5.

## 4. Results

This chapter presents the results of the two methods employed in QGIS; the temporal controller method and the IDW interpolation method respectively.

The temporal controller in QGIS allows for an animation to be created from the data. Unfortunately, an animation cannot be included here, so for the purpose of presenting the results in this thesis, the maps in figure 4 are snapshots of this time series animation. They are presented in chronological order from oldest to younger, and the number of burials in each map is noted underneath the snapshots. The first map shows the two oldest sites from before 2900 BC. Each subsequent snapshot covers a time period of 50 years until 2200 BC. The number of sites accumulates throughout the snapshots until the total number of selected burials is reached in map number 15.

The series of 25 maps created using the IDW interpolation method are similarly presented, as shown in figure 5. They are again presented from oldest to youngest, with a time interval of 50 years. Because the probability radiocarbon data covers a larger time span than the mean radiocarbon dates used in the previous map series, the resulting number of maps is higher.



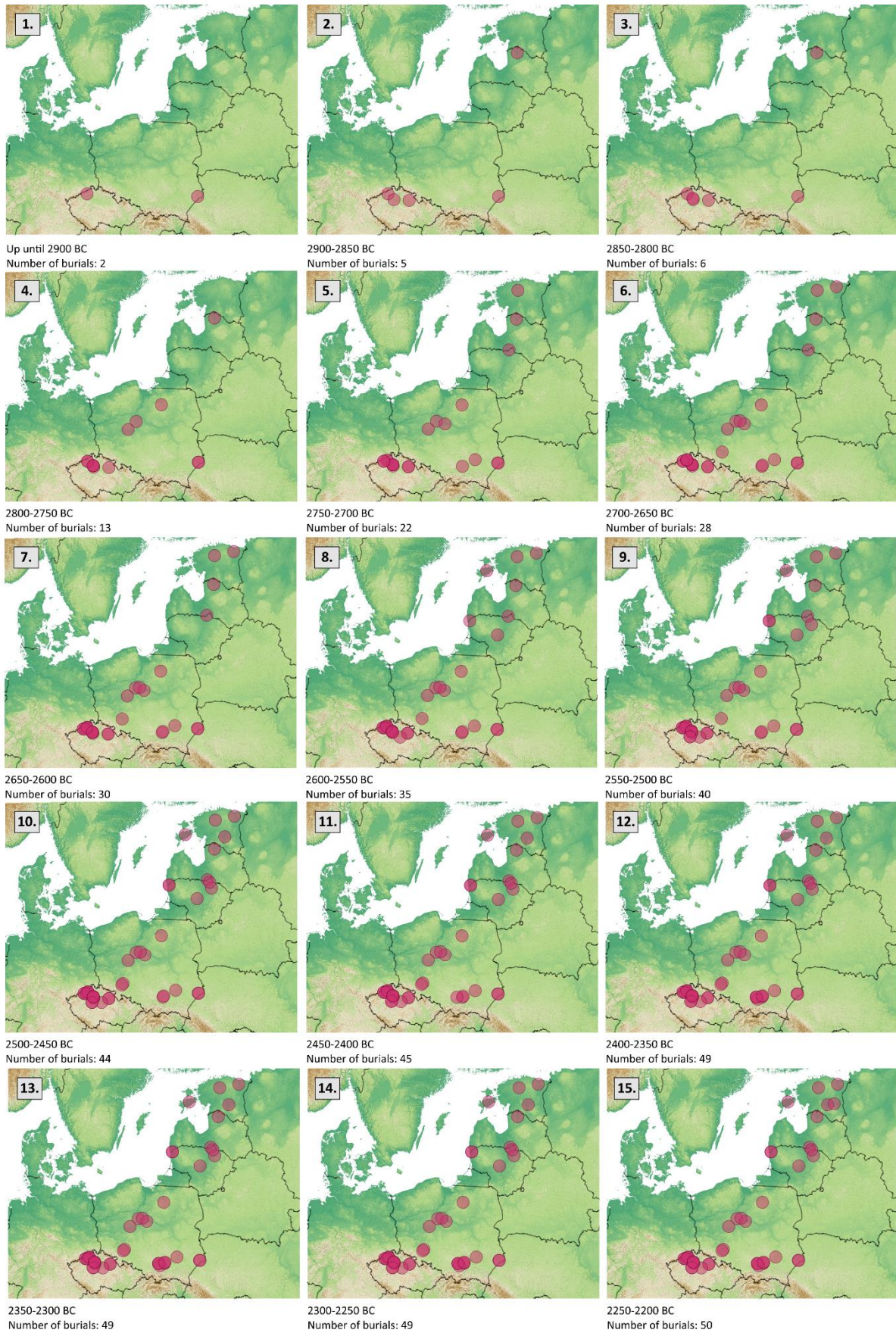


**Figure 4** Maps of the research area as snapshots from the temporal controller animation. The maps are numbered 1 through 12 and the time range and number is burials is noted underneath each map (maps by Alissa Grave made in QGIS).



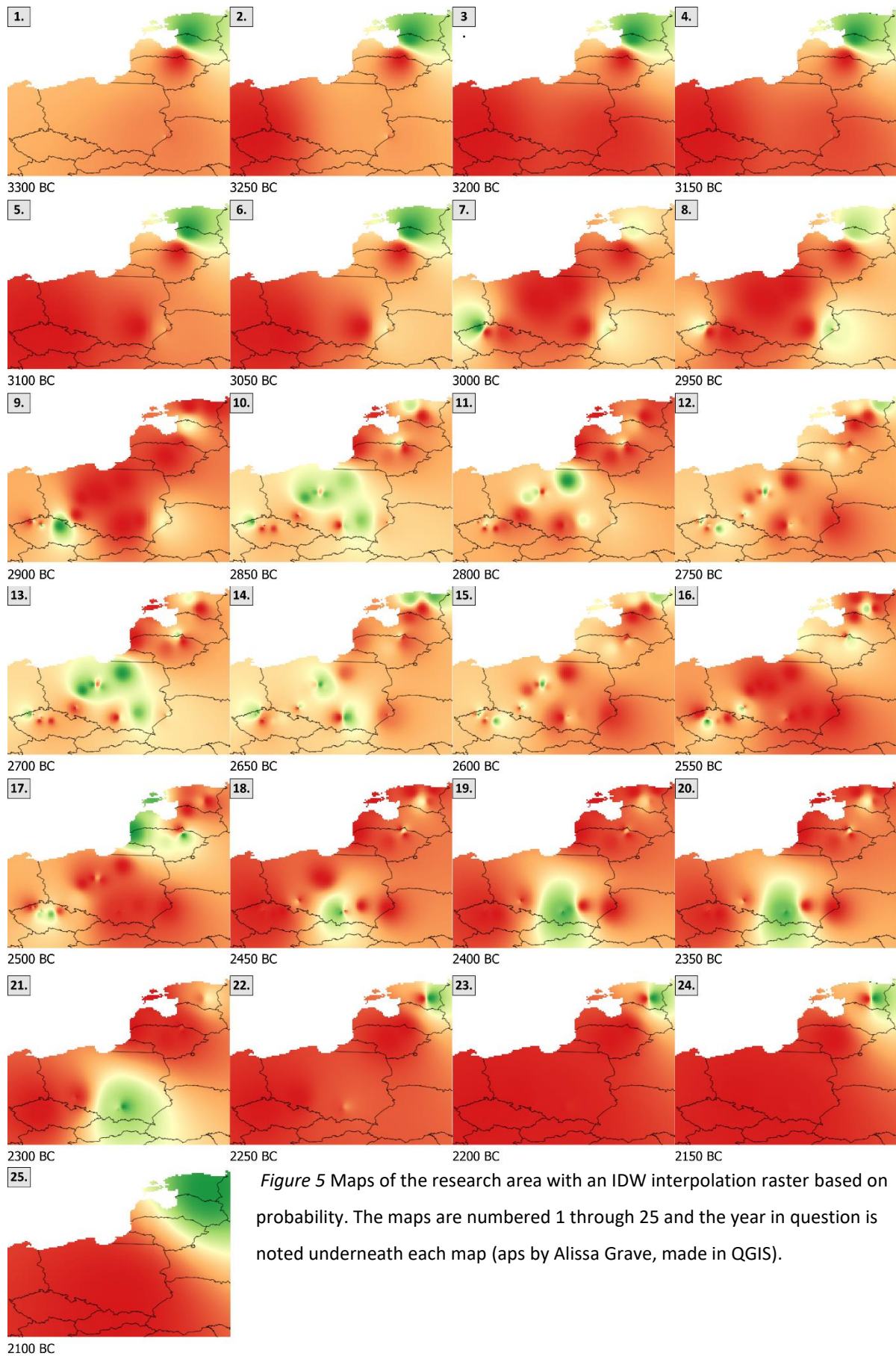


*Figure 5* Maps of the research area with an IDW interpolation raster based on probability. The maps are numbered 1 through 25 and the year in question is noted underneath each map (aps by Alissa Grave, made in QGIS).

## 5. Discussion

This chapter carefully evaluates the results presented in the previous chapter, and primarily address the last three of the five sub-questions. A comparison will be made between the interpretations of the two methods used in QGIS. The results will furthermore be discussed in relation to some of the existing theoretical ideas about the movement of Corded Ware culture.

### 5.1. Temporal controller maps interpretation

Looking at the first series of maps created using the temporal controller (figure 4), the oldest burials are found in the Czech Republic and southern Poland. Wereszczyca1 in southeastern Poland is the oldest date in the data set (2938 BC), but it is soon followed by a couple of Czech burials.

Interestingly, Zvejnieki137 in northern Latvia is the fourth oldest burial (2983 BC), despite its geographical distance from the three oldest burials. The second and third oldest Corded Ware burial of the Eastern Baltics do not show up until map 5 (2743 BC), meanwhile about twelve additional burials have appeared in the Czech Republic and Poland. From that point onward until map number 10 (2450 BC), the number of additional sites per map increases pretty steadily and somewhat evenly across the whole research area; new burials are showing up in the Eastern Baltics as well as in the Czech Republic and Poland. Only Polish burials are added between map number 11 and 12.

Interestingly, no change happens between map number 12 and 14 (2400-2250 BC), as the number of burials remains 49. The last and most recent burial according to these maps is Karlova1 in Estonia (2246 BC), which is added in map number 15.

### 5.2 IDW interpolation maps interpretation

The second series of maps, created using IDW interpolation (figure 5), starts off with several maps showing a single very high probability area in the Eastern Baltics, caused by the Zvejnieki137 site. Very clear high probability areas do not show up in Poland and the Czech republic until around map number 7 (-3200 BC). Map number 7 is also where this high probability area in the Eastern Baltics starts to reduce. It is between map number 9 and 11 (2900-2800 BC) where an expansion further north into the rest of Poland could be interpreted. It is notable that map number 10 and 13 (2850-2700 BC) look very similar in terms of probability in both Poland and the Czech Republic. There are some red spots mixed in that represent the older dates in the Czech Republic and southern Poland, which have a lower or zero probability by this time. Between map 10 and 16 the probability in the Eastern Baltics fluctuates a bit, marking different sites with different ages. Most of Poland turns red again by map number 16 (2550 BC), while an area in the Eastern Baltics peaks in probability on map number 17 (2500 BC) before turning red again. From map number 18 to 21 (2450-2300 BC), one

primary high probability area exists in southern Poland, which disappears almost completely in map number 22 (2250 BC). At the same time, a single high probability area in the Eastern Baltics shows up, representing the Karlova1 site in Estonia, which endures high until the final map.

### 5.3 Interpretation side by side

The Zvejnieki137 burial in Latvia appears more prominently before any other sites in the IDW maps (map number 1-6), and appears as the fourth burial in the temporal controller maps (map number 2). Either way, it is a notable early burial in both series considering how the rest of the burials in the Eastern Baltics appear later on in each series. Like mentioned in chapter, Zvejnieki137 is a burial that has previously been suspected of being affected by the freshwater reservoir effect. While the FRE would explain why this burial has a very early date, it has been shown that the burial is unlikely to be affected (Meadows et al., 2014, p. 830), making it quite a remarkable outlier. Such outlier result can be regarded as very significant. For example, they could suggest very high degrees of mobility within a very short period of time or an entirely different migration route. However, suggesting a chronological model with all dates taken into consideration can be risky. In one case, a very early date for a Corded Ware burial in Poland was taken as evidence of a very early chronology, but was later corrected by a second dating (Włodarczak, 2009, p. 742-743). Changing the overarching theory for the sake of one burial was deemed too risky in this thesis.

Overall, despite some subtle differences, both of the series of maps share a degree of similarity. The most important similarity is that they can both be interpreted to show a northward movement. There is certainly Corded Ware activity in the Czech Republic and Poland before most of the Eastern Baltic activity, as can be best seen in maps 4-5 in the temporal controller series, and map 9-11 in the IDW interpolation series. The last burial, prominent in both map series, is also the same burial in the Eastern Baltics. The rough area around southern Poland and Bohemia in the Czech republic can therefore be interpreted as core areas from where Corded Ware moved up. In this interpretation, it was decided to not interpret another core area in the Eastern Baltics to accommodate the single site of Zvenjnieki137, for the reasons stated above.

### 5.4 Comparison of models

The results of this thesis can be compared to existing theoretical models or suggestions for the spread of Corded Ware culture. The first model discussed here was formulated by Nordqvist & Heyd in a 2020 paper on the Fatyanovo Culture of Russia, which the authors argues is part of the Corded Ware family. This model suggests that the emergence of the Fatyanovo Culture was the result of an eastward movement of Corded Ware people from the Eastern Baltics, into a part of Russia where no

(Nordqvist & Heyd, 2020, p. 84-85). In a wider picture of the distribution of key cultures, they suggest a looping movement starting with the Yamnaya moving westward from the Pontic-Caspian steppes, then continuing up north into central Europe and the Baltics and then back to the east to the Russian region where Fatyanovo can be found (figure 6). Assuming this model is correct, a northward movement within the research area of this thesis would be expected. This fits the interpretation of the data that was discussed in chapter 5.3.

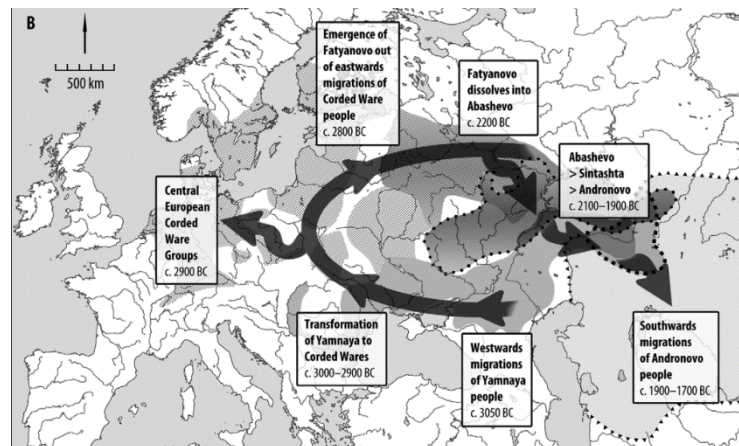


Figure 6 A model based on a Baltic origin for the Fatyanovo Culture in Russia. The movement of Corded Ware loops clockwise through Europe (map taken from Nordqvist & Heyd, 2020, p. 84).

Papac et al. proposed another potential model in a 2021 paper, based on genetic research. They found that a northeastern European forest steppe ancestry possibly contributed to early Corded Ware groups (Papac et al., 2021, p. 9-10). This would imply that a movement of people took place not only from the Pontic-Caspian steppes, but additionally from the forest steppe areas of northeastern Europe, which covers a large part of the research area (see figure 7). Both of these movements are eastward, so an eastward movement would be expected in this thesis' research area as well, which does not line up with the interpretation in this thesis. The authors do emphasize that northeastern Europe is as of yet poorly sampled for ancient DNA (Papac et al., 2021, p. 10).



Figure 7 A model based on potential forest steppe ancestry in Corded Ware people. The arrival of forest steppe ancestry is shown as another westward movement (map taken from Papac et al., 2021, p. 9).

A third model from a paper by Haak et al. (2015) is also based on genetic evidence from ancient DNA. Their research documents a migration wave around 4500 years ago that resulted in the presence of high percentages of steppe ancestry in Corded Ware populations. They also relate this migration to the steppe hypothesis, a theory on language dispersal which proposes that early speakers of Indo-European languages from the steppes came to Europe following the invention of the wheel (Haak et al., 2015, p. 211). Based on this, a somewhat simple model moving from southeast to northwest was given, as seen in figure 8. Southeast to northwest does not perfectly align with this thesis's interpretation of the results.

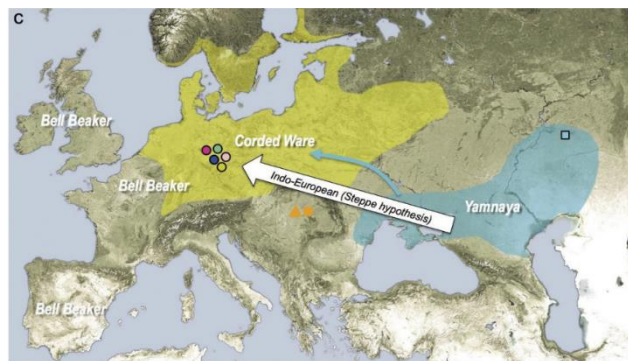


Figure 8 A model based on genetic evidence. This evidence was linked to the steppe hypothesis by the authors (map taken from Haak et al., 2015).

All three of these models still consider the Pontic-Caspian steppes as at least a partial region of origin for what would later become the Corded Ware culture, but how Corded Ware moved after their potential ancestors departed from the steppes varies. The model by Nordqvist & Heyd would fit the results found in this thesis the best, followed by the model by Haak et al., and then Papac et al.

## 5.5 Limitations

Both methods employed in QGIS admittedly have their limitations. Regarding the temporal controller method, a mean ( $\mu$ ) of each calibrated date was used to pinpoint a date. It is important to note that it is quite likely that this singular date is not when each burial actually occurred. Calibrated probability distributions cover many years and can have several peaks of higher probability. The mean age, by its nature, could technically fall perfectly in between any high probability peaks. The IDW interpolation method does take into account the full probability distribution of each burial, but the interpolation comes with its own issues. IDW interpolation is a method that is known to have a tendency to create local extrema at data points (Mitas & Mitasova, 2005, p. 482-483). This does seem to be happening in the maps presented here too, as high probability is very visually prominent

and so is a low probably. Low and high probabilities do occur in close proximity to each other on the maps, and can make the maps a bit harder to read.

Lastly, 50 burials is still a pretty small dataset considering the geographical and temporal range of the Corded Ware culture. While it was necessary to deselect a number of burials for the sake of certainty and accuracy, a larger dataset of C14 dates with a similar level of accuracy could result in a more refined result. Increasing availability of such large digital datasets in recent times certainly give hope for more extensive research into human population change using radiocarbon data in the future (Crema et al., 2017, p. 7), which could include the spread of Corded Ware culture.



## 6. Conclusion

This thesis has made an attempt to visualize the spatiotemporal spread of Corded Ware burial practices. Here follows the answers to the questions posed at the beginning, along with suggestions for future research.

### 6.1 Findings

1. What criteria should be used to select reliable radiocarbon-dated Corded Ware burial sites in the research area?

Most of the criteria, as described in further detail in chapter 3.1, are related to the sample used for radiocarbon dating and its context. This includes that the sample needed to be taken from material inside of the grave pit and that at least a couple reliable Corded Ware elements needed to be present in the context of the sample. A few common problems with radiocarbon dating were also addressed. Two cases in which the freshwater reservoir effect seemed to be relevant at first were still able to be included based on other researchers' work. A maximum standard deviation was also defined at 60 years. All criteria were chosen based on adhering to a certain level of certainty and accuracy, while taking into account that having criteria that are too strict can narrow down the data too much to use for a proper analysis.

2. What spatiotemporal GIS method is most suitable for mapping the selected burial sites in QGIS?

Two methods were employed within QGIS to map the selected burial sites. One method involved the use of the temporal controller, resulting in an animation that showed the accumulating appearance of Corded Ware burials in the research area. The second method focused on the use of inverse distance weighting (IDW) interpolation based on the full probability distribution of each calibrated date. A general trend of a northward movement can be interpreted in the results of both methods. This was perhaps slightly easier to observe in the temporal controller results, but unlike the IDW method, it does not consider the full probability distribution. Both methods admittedly come with limitations, and the more suitable method depends on priorities. It is also important to note that there are many other methods outside of the ones that this thesis explored (see chapter 6.2).

3. According to the spatiotemporal maps, where can we identify the oldest core area (or areas) where Corded Ware culture originated from within the research area?

The oldest core areas according to both of the QGIS methods are in the Czech Republic (specifically in the region of Bohemia) and southern Poland. One specific outlier in northern Latvia could be seen as part of an additional core area in the Eastern Baltics, but this is a risky assumption to make based

on one piece of data, as it would have major consequences for how movement of Corded Ware culture could be interpreted in the research area. Therefore, this paper does not define it as a core area.

4. According to the spatiotemporal maps, what is the direction of movement out of this core area (or areas)?

Both map series can be interpreted to show a general northward movement from the core areas in the Czech Republic and Poland up into the Eastern Baltics. Like stated above, the outlier in Latvia does not fit into this pattern. If it were counted as a core area, it could be argued that a very high degree of mobility is visible, or that no clear direction of movement came out of the results at all.

5. How do the patterns that emerge from the spatiotemporal GIS maps compare to existing models for the movement of Corded Ware culture during the 3<sup>rd</sup> millennium BC?

In chapter 5.2, three different theoretical models for the movement of Corded Ware culture were compared to this thesis' result. Only one of these models is truly compatible with the northward movement observed in the results, which is the model based on an Eastern Baltic origin for the Fatyanovo culture in Russia by Nordqvist & Heyd (2020). The other two by Papac et al. (2020) and Haak et al. (2015) are based on ancient DNA, are interestingly less compatible.

On the basis of these answers, the main research question of this thesis can be answered:

- What was the spatiotemporal spread of Corded Ware burial practices in the Czech Republic, Poland, and the Eastern Baltics during the 3<sup>rd</sup> millennium BC?

The spatiotemporal spread in the research area during the 3<sup>rd</sup> millennium BC, according to the results achieved and discussed in this study, can be described as following a northward movement from a core area around the Czech Republic and southern Poland, although an outlier in Latvia exists. These results are more or less in line with some theoretical ideas within academia for Corded Ware migration, but not all. Within the scope of this thesis, only two different GIS methods were employed, each with their own limitations. Other spatiotemporal methods as well as a larger amount of high quality data could certainly refine the results.

## 6.2 Future directions

While this thesis does not delve into potential motivations for the movement of Corded Ware culture, nor about the manner of movement, these topics are indeed relevant for any discussion on the movement of populations or the spread of a culture. Questions one might ask include the following. What were the environmental and ecological factors and that influenced the spread of



Corded Ware culture? What social and cultural factors played a role? What were the long term consequences of the spread of Corded Ware culture for other local cultures or neighboring cultures? Any model for the spread of Corded Ware, including those based on spatiotemporal methods like the one presented here and any future spatiotemporal research, needs to be compatible with findings regarding these sort of questions and vice versa.

Regarding spatiotemporal methods themselves, there is a lot more that can be done. Only two methods have been explored here, and the interpolation method used in this research is just one of several interpolation methods, including kriging, splines, TIN interpolation, heatmaps, et cetera. A least-cost distance model starting from the core areas could also have interesting results, as it would take into account external factors of the landscape. Comparing the results of a wide range of spatiotemporal methods could potentially lead to bigger conclusions and therefore bigger contributions to the debate at hand.

Like previously mentioned, a larger data set would no doubt also help achieve promising results in any quantitative method, and the amount of data available only grows with time. The author of this thesis is therefore looking forward to future developments in the realm of Corded Ware.

## Bibliography

- Allentoft, M. E., Sikora, M., Sjögren, K.-G., Rasmussen, S., Rasmussen, M., Stenderup, J., Damgaard, P. B., Schroeder, H., Ahlström, T., Vinner, L., Malaspinas, A.-S., Margaryan, A., Higham, T., Chivall, D., Lynnerup, N., Harvig, L., Baron, J., Casa, P. D., Dąbrowski, P., ... Willerslev, E. (2015). Population genomics of Bronze Age Eurasia. *Nature*, *522*(7555), 167–172. <https://doi.org/10.1038/nature14507>
- Baron, J., Furmanek, M., Hałaszkó, A., & Kufel-Diakowska, B. (2019). Differentiation of burial practices in the Corded Ware Culture. The example of the Magnice site in SW Poland. *Præhistorische Zeitschrift*, *93*(2), 169–184. <https://doi.org/10.1515/pz-2018-0009>
- Bourgeois, Q., & Kroon, E. (2017). The impact of male burials on the construction of Corded Ware identity: Reconstructing networks of information in the 3rd millennium BC. *PLOS ONE*, *12*(10), e0185971. <https://doi.org/10.1371/journal.pone.0185971>
- Champion, T., Clive, G., Shennan, S., & Whittle, A. (2009). Settlement expansion and socio-economic change 3200-2300 BC. In *Prehistoric Europe*. Routledge.
- Crema, E. R., Bevan, A., & Shennan, S. (2017). Spatio-temporal approaches to archaeological radiocarbon dates. *Journal of Archaeological Science*, *87*, 1–9. <https://doi.org/10.1016/j.jas.2017.09.007>
- Discover QGIS. (n.d.). Retrieved April 28, 2023, from <https://qgis.org/en/site/about/index.html>
- Dobeš, M., Pecinová, M., & Ernée, M. (2021). On the earliest Corded Ware in Bohemia. In V. Heyd, G. Kulcsár, & B. Preda-Bălănică (Eds.), *Yamnaya Interactions: Proceedings of the International Workshop held in Helsinki, 25-26 April 2019* (Vol. 2). Archaeolingua.
- Download QGIS. (n.d.). Retrieved June 2, 2023, from <https://www.qgis.org/en/site/forusers/download.html>
- Editable GeoCSV — QGIS Python Plugins Repository. (n.d.). Qgis.Org. Retrieved April 16, 2023, from <https://plugins.qgis.org/plugins/editablegeocsv/>

- Furholt, M. (2003). *Die absolutchronologische Datierung der Schnurkeramik in Mitteleuropa und Südkandinavien*. Dr. Rudolf Habelt GmbH.
- Furholt, M. (2014). Unpending a 'totality': Re-evaluating Corded Ware variability in Late Neolithic Europe. *Proceedings of the Prehistoric Society*, 80, 67–86.  
<https://doi.org/10.1017/ppr.2013.20>
- Furholt, M. (2019). Re-integrating archaeology: A contribution to aDNA Studies and the migration discourse on the 3rd millennium BC in Europe. *Proceedings of the Prehistoric Society*, 85, 115–129. <https://doi.org/10.1017/ppr.2019.4>
- Furholt, M. (2020). Social Worlds and Communities of Practice: A polythetic culture model for 3rd millennium BC Europe in the light of current migration debates. *Préhistoires Méditerranéennes*, 8. <https://doi.org/10.4000/pm.2383>
- Google Maps. (n.d.). Google Maps. Retrieved June 2, 2023, from  
<https://www.google.com/maps/@52.2716959,6.23128,14z?entry=ttu>
- Graser, A. (2020, May 10). TimeManager is dead, long live the Temporal Controller! *Free and Open Source GIS Ramblings*. <https://anitagraser.com/2020/05/10/timemanager-is-dead-long-live-the-temporal-controller/>
- Haak, W., Lazaridis, I., Patterson, N., Rohland, N., Mallick, S., Llamas, B., Brandt, G., Nordenfelt, S., Harney, E., Stewardson, K., Fu, Q., Mittnik, A., Bánffy, E., Economou, C., Francken, M., Friederich, S., Pena, R. G., Hallgren, F., Khartanovich, V., ... Reich, D. (2015). Massive migration from the steppe was a source for Indo-European languages in Europe. *Nature*, 522(7555), 207–211. <https://doi.org/10.1038/nature14317>
- Heyd, V. (2021). Yamnaya, Corded Wares, and Bell Beakers on the move. In V. Heyd, G. Kulcsár, & B. Preda-Bălănică (Eds.), *Yamnaya Interactions: Proceedings of the International Workshop held in Helsinki, 25-26 April 2019* (Vol. 2). *Archaeolingua*.
- Ikechukwu, M. N., Ebinne, E., Idorenyin, U., & Raphael, N. I. (2017). Accuracy assessment and comparative analysis of IDW, spline and kriging in spatial interpolation of landform

- (topography): An experimental study. *Journal of Geographic Information System*, 09(03), 354–371. <https://doi.org/10.4236/jgis.2017.93022>
- Lõugas, L., Kriiska, A., & Maldre, L. (2007). New dates for the Late Neolithic Corded Ware Culture burials and early husbandry in the East Baltic region. *Archaeofauna*, 16.
- Meadows, J., Bērziņš, V., Brinker, U., Lübke, H., Schmölcke, U., Staude, A., Zagorska, I., & Zariņa, G. (2016). Dietary freshwater reservoir effects and the radiocarbon ages of prehistoric human bones from Zvejnieki, Latvia. *Journal of Archaeological Science: Reports*, 6, 678–689. <https://doi.org/10.1016/j.jasrep.2015.10.024>
- Meadows, J., Lübke, H., Zagorska, I., Berziņš, V., Ceriņa, A., & Ozola, I. (2014). Potential Freshwater Reservoir Effects in a Neolithic Shell Midden at Riņņkalns, Latvia. *Radiocarbon*, 56(2), 823–832. <https://doi.org/10.2458/56.16950>
- Mitas, L., & Mitasova, H. (2005). Spatial Interpolation. In P. A. Longley, M. F. Goodchild, D. J. Maguire, & D. W. Rhind (Eds.), *Geographic Information Systems: Principles, Techniques, Management and Applications* (2nd ed.). Wiley.
- Mittnik, A., Wang, C.-C., Pfrengle, S., Daubaras, M., Zariņa, G., Hallgren, F., Allmäe, R., Khartanovich, V., Moiseyev, V., Tõrv, M., Furtwängler, A., Andrades Valtueña, A., Feldman, M., Economou, C., Oinonen, M., Vasks, A., Balanovska, E., Reich, D., Jankauskas, R., ... Krause, J. (2018). The genetic prehistory of the Baltic Sea region. *Nature Communications*, 9, 442. <https://doi.org/10.1038/s41467-018-02825-9>
- Monmonier, M. (1990). Strategies for the visualization of geographic time-series data. *Cartographica: The International Journal for Geographic Information and Geovisualization*, 27(1), 30–45. <https://doi.org/10.3138/U558-H737-6577-8U31>
- Natural Earth. (n.d.). *Admin 0 – Boundary Lines*. Retrieved April 9, 2023, from <https://www.naturalearthdata.com/downloads/10m-cultural-vectors/10m-admin-0-boundary-lines/>

- Nederlandse Organisatie voor Wetenschappelijk Onderzoek. (n.d.). *The Talking Dead. Reconstructing the transmission of information in Corded Ware and Bell Beaker societies during the 3rd Millennium BC*. <https://www.nwo.nl/projecten/vividi191149>
- Nordqvist, K., & Heyd, V. (2020). The forgotten child of the wider Corded Ware family: Russian Fatyanovo Culture in context. *Proceedings of the Prehistoric Society*, 86, 65–93.  
<https://doi.org/10.1017/ppr.2020.9>
- Papac, L., Ernée, M., Dobeš, M., Langová, M., Rohrlach, A. B., Aron, F., Neumann, G. U., Spyrou, M. A., Rohland, N., Velemínský, P., Kuna, M., Brzobohatá, H., Culleton, B., Daněček, D., Danielisová, A., Dobisíková, M., Hložek, J., Kennett, D. J., Klementová, J., ... Haak, W. (2021). Dynamic changes in genomic and social structures in third millennium BCE central Europe. *Science Advances*, 7(35), eabi6941. <https://doi.org/10.1126/sciadv.abi6941>
- Pospieszny, Ł. (2015). Freshwater reservoir effect and the radiocarbon chronology of the cemetery in Żąbnie, Poland. *Journal of Archaeological Science*, 53, 264–276.  
<https://doi.org/10.1016/j.jas.2014.10.012>
- Racimo, F., Woodbridge, J., Fyfe, R. M., Sikora, M., Sjögren, K.-G., Kristiansen, K., & Vander Linden, M. (2020). The spatiotemporal spread of human migrations during the European Holocene. *Proceedings of the National Academy of Sciences*, 117(16), 8989–9000.  
<https://doi.org/10.1073/pnas.1920051117>
- Taylor, R.E., & Bar-Yosef, O. (2016). *Radiocarbon Dating: An Archaeological Perspective* (2nd ed.). Routledge. <https://doi.org/10.4324/9781315421216>
- Reimer, P. J., Austin, W. E. N., Bard, E., Bayliss, A., Blackwell, P. G., Bronk Ramsey, C., Butzin, M., Cheng, H., Edwards, R. L., Friedrich, M., Grootes, P. M., Guilderson, T. P., Hajdas, I., Heaton, T. J., Hogg, A. G., Hughen, K. A., Kromer, B., Manning, S. W., Muscheler, R., ... Talamo, S. (2020). The IntCal20 northern hemisphere radiocarbon age calibration curve (0–55 cal kBP). *Radiocarbon*, 62(4), 725–757. <https://doi.org/10.1017/RDC.2020.41>

- Scott, E. M., & Reimer, P. J. (2009). Calibration introduction. *Radiocarbon*, 51(1), 283–285.  
<https://doi.org/10.1017/S0033822200033816>
- Taylor, R. E., & Bar-Yosef, O. (Eds.). (2016). *Radiocarbon Dating: An Archaeological Perspective* (2nd ed.). Routledge.
- Terrestris. (2019, January 29). *Digital elevation model SRTM30 WMS*.  
<https://www.terrestris.de/en/hoehenmodell-srtm30-wms/>
- TimeManager—QGIS Python Plugins Repository*. (n.d.). Retrieved June 2, 2023, from  
<https://plugins.qgis.org/plugins/timemanager/>
- Vander Linden, M. (2007). For equalities are plural: Reassessing the social in Europe during the third millennium BC. *World Archaeology*, 39(2), 177–193.  
<https://doi.org/10.1080/00438240701249678>
- WGS 84 / Pseudo-Mercator—Spherical Mercator, Google Maps, OpenStreetMap, Bing, ArcGIS, ESRI - EPSG*. (n.d.). Retrieved May 29, 2023, from <https://epsg.io>
- WGS 84—WGS84—World Geodetic System 1984, used in GPS - EPSG*. (n.d.). Epsg.io. Retrieved May 29, 2023, from <https://epsg.io>
- Włodarczak, P. (2009). Radiocarbon and Dendrochronological Dates of the Corded Ware Culture. *Radiocarbon*, 51(2), 737–749. <https://doi.org/10.1017/S003382220005606X>

## **Abstract**

The Yamnaya of the Pontic-Caspian steppe have long been assumed to be responsible for the emergence of the Corded Ware culture as they moved westward into Europe. Recent research, especially in the field of ancient DNA, add nuance to this assumption. While certain cultural elements between the Yamnaya and Corded Ware culture are similar, Corded Ware individuals were shown to have varying amounts of steppe ancestry. In light of this discussion, where Corded Ware culture first appeared and how it spread across large parts of continental Europe according to quantitative spatiotemporal methods could provide a valuable contribution. The Czech Republic, Poland, and the Eastern Baltic countries together form a key area that can be seen as a corridor for the movement of Corded Ware culture. Fifty radiocarbon dated samples from Corded Ware burial sites in this research area were carefully selected from a larger data set to ensure a balance of quality and quantity. These dates were then calibrated and prepared for use in the open-source geographic information systems (GIS) software QGIS. The data was visualized in two distinct ways, one method involved the temporal controller panel, while the other used inverse distance weighting (IDW) interpolation. This resulted in two series of maps; 15 maps consisting of snapshots of the temporal controller animation that used the mean calibrated date of each sample, and 25 maps with interpolation raster layers that used the full probability range of each calibrated date. Both of the resulting series of map can be interpreted to show core areas in the Czech Republic and southern Poland and a general northward movement, though one specific surprisingly old burial is located in Latvia. This burial was chosen to be omitted in this case, as it was deemed risky to include when looking for patterns. After comparing the results to three other theoretical models for the movement of Corded Ware, the interpretation of a northward migration could support one of them but not necessarily the other two, which happened to be based on ancient DNA. The results of this thesis are perhaps just the start of a future in which further research with other spatiotemporal methods and larger data sets can significantly contribute to the debate on Corded Ware massive migrations.

## List of Figures

Cover figure	0
<hr/>	
<a href="https://www.mapchart.net/europe.html">https://www.mapchart.net/europe.html</a>	
Rudnicki, M., & Włodarczak, P. (2007). Graves of the Corded Ware culture at the multicultural site 6 in Pełczyska, district of Pińczow. <i>Sprawozdania Archeologiczn</i> , 59.	
Figure 1	8
<hr/>	
The research area indicated in green on a map of Europe. The countries are adjacent to one another ( <a href="https://www.mapchart.net/europe.html">https://www.mapchart.net/europe.html</a> ).	
Figure 2	15
<hr/>	
Two examples of different looking calibration plots in OxCal v4.4.4. Grave 137 at the Zvejnieki site in Latvia (Zvejnieki137) has a mean ( $\mu$ ) calibrated age of 2893 BC, and grave 67/87 at the Stadice site in the Czech Republic (STD003) has a mean ( $\mu$ ) calibrated age of 2927 BC ( <a href="https://c14.arch.ox.ac.uk/oxcal/OxCal.html#">https://c14.arch.ox.ac.uk/oxcal/OxCal.html#</a> ).	
Figure 3	18
<hr/>	
A snippet of the data report exported by OxCal containing detailed probability data. This shows only the probability of the years -2879.5 to -2754 of grave 1 at the Smrokow site in Poland ( <a href="https://c14.arch.ox.ac.uk/oxcal/OxCal.html#">https://c14.arch.ox.ac.uk/oxcal/OxCal.html#</a> ).	
Figure 4	22
<hr/>	
Maps of the research area as snapshots from the temporal controller animation. The maps are numbered 1 through 12 and the time range and number of burials is noted underneath each map (maps by Alissa Grave made in QGIS).	
Figure 5	23
<hr/>	
Maps of the research area with an IDW interpolation raster based on probability. The maps are numbered 1 through 25 and the year in question is noted underneath each map (maps by Alissa Grave, made in QGIS).	
Figure 6	26
<hr/>	
A model based on a Baltic origin for the Fatyanovo Culture in Russia. The movement of Corded Ware loops clockwise through Europe (map taken from Nordqvist & Heyd, 2020, p. 84).	
Figure 7	26
<hr/>	
A model based on potential forest steppe ancestry in Corded Ware people. The arrival of forest steppe ancestry is shown as another westward movement (map taken from Papac et al., 2021, p. 9).	
Figure 8	27
<hr/>	
A model based on genetic evidence. This evidence was linked to the steppe hypothesis by the authors (map taken from Haak et al., 2015).	



# Appendix A

Table containing the data of all the selected Corded Ware burials

ID	Country	Region	Site name	Grave nr.	Latitude	Longitude	Culture	Lab. nr.	OGIS dates	Calibr. BC	C14 BP	s.d.	Sample	Direct/Indirect	Sources
Karłowa1	Estonia		Karłowa	1	58.37254	26.72322	CWC	Poz-15099	2754-01-01	-2246	3805	35	human bone (mandibula)	direct	Malmström et al. 2019; Kriska et al. 2007
Pelczyńska	Poland	Lesser Poland	Pelczyńska 6	32/2002	50.35675	20.56803	CWC	Poz-12580	2638-01-01	-2362	3880	35	human bone	direct	Jaros & Włodarczak 2007; Rudnicki & Włodarczak 2007
Smokow	Poland	Lesser Poland	Smokow 17	2	50.28545	20.0308	CWC	Poz-9588	2653-01-01	-2367	3885	35	human bone	direct	Jaros & Włodarczak 2007; Włodarczak 2004
Zielona	Poland	Lesser Poland	Zielona 3	7	50.15972	20.15053	CWC	Poz-9577	2620-01-01	-2386	3895	35	human bone	direct	Jaros & Włodarczak 2007; Włodarczak 2004
Smokow	Poland	Lesser Poland	Smokow 17	10	50.28545	20.0308	CWC	Poz-9584	2614-01-01	-2380	3905	35	human bone	direct	Jaros & Włodarczak 2007; Włodarczak 2007
Smokow	Poland	Lesser Poland	Smokow 17	7	50.28545	20.0308	CWC	Poz-9600	2654-01-01	-2448	3950	35	human bone	direct	Jaros & Włodarczak 2007; Włodarczak 2007
Birza1	Lithuania		Birza1	1	56.207306	24.61057	CWC/Battle Ave culture	Poz-64678	2534-01-01	-2466	3950	30	human bone	direct	Mittnik et al. 2018; Pilliciauskas et al. 2017; Pilliciauskas et al. 2018
Kunila2	Estonia		Kunila	2	58.325533	26.152339	CWC	Poz-10825	2533-01-01	-2467	3960	40	human bone (mandibula)	direct	Mittnik et al. 2018; Kriska et al. 2007
Magnice8	Poland		Magnice8	46A	50.98863	16.95951	CWC	Poz-26510	2514-01-01	-2486	3970	40	human bone	direct	Baron et al. 2019
VIL020	Czech Republic	Bohemia	Vilavěves	Grave 9730	50.365945	14.446606	LCW	MAMS-30761	2403-01-01	-2497	3966	25	human bone	direct	Papac et al. 2021
OH001	Czech Republic	Bohemia	Práha - Malá Ohrada	Grave 10	50.04618	14.37021	LCW	MAMS-44769	2482-01-01	-2518	3987	25	human bone	direct	Papac et al. 2021; Buchvaldek & Kovarik 1993
OH002	Czech Republic	Bohemia	Práha - Malá Ohrada	Grave 26	50.04618	14.37021	LCW	MAMS-41374	2477-01-01	-2528	4017	25	human bone	direct	Papac et al. 2021
VIL010	Czech Republic	Bohemia	Vilavěves	Grave 1423	50.365945	14.446606	MCW	MAMS-38472	2465-01-01	-2534	4027	25	human bone	direct	Papac et al. 2021
Benalcañ1	Lithuania		Benalcañ1	1	56.1021	21.228051	CWC	Poz-66923	2462-01-01	-2538	4025	30	skull	direct	Pilliciauskas et al. 2017b
Gyskera1	Lithuania		Gyskera1	1	55.917796	24.913053	CWC/Battle Ave culture	Poz-61584	2457-01-01	-2543	4030	30	human bone (fibula, adult male)	direct	Mittnik et al. 2018; Pilliciauskas et al. 2017; Tebeikis & Jankauskas 2002
Benalcañ3	Lithuania		Benalcañ3	3	56.1021	21.228051	CWC	Poz-61591	2444-01-01	-2556	4040	30	skull	direct	Pilliciauskas et al. 2017b
Tika	Estonia		Tika	1	58.456498	22.708818	CWC	Poz-10803	2437-01-01	-2557	4035	35	human bone (mandibula)	direct	Kriska et al. 2007
OB004.A.B	Czech Republic	Bohemia	Obfistvi	Grave 372	50.292725	14.484945	MCW	MAMS-38483	2437-01-01	-2563	4048	26	human bone	direct	Papac et al. 2021; Pecinovsky
Plinkaigalis241	Lithuania		Plinkaigalis	241	55.410218	23.646787	CWC/Battle Ave culture	OVA-5928	2421-01-01	-2579	4030	55	human bone?	direct	Mittnik et al. 2018; Antanaitis-Jacobs et al. 2009
KO1002.A	Czech Republic	Bohemia	Kolin L7b	Grave 3013	50.033343	15.168084	CW	MAMS-38481	2416-01-01	-2584	4055	29	human bone	direct	Papac et al. 2021; preliminary reports in: Sumbereva et al. 2010; Sumbereva et al. 2012
VIL009	Czech Republic	Bohemia	Vilavěves	Grave 965	50.365945	14.446606	CW	MAMS-45797	2364-01-01	-2636	4078	25	human bone	direct	Papac et al. 2021
RDV001	Czech Republic	Bohemia	Radovesice XVI	Grave 41/83	50.543303	13.843248	MCW	MAMS-45796	2357-01-01	-2643	4081	25	human bone	direct	Papac et al. 2021; Dobeš et al. 1991
Jagodno	Poland	Silesian Lowland	Jagodno	Feature 1	51.063363	17.066138	CWC	Poz-259596	2346-01-01	-2654	4080	40	human bone	direct	Gworys et al. 2011
Kuczkowo	Poland	Kujawy	Kuczkowo	Grave 10/87	52.7416	18.62049	CWC	OxA-26755	2341-01-01	-2659	4086	29	human bone	direct	Czebreszuk 2000; Pospieszny et al. 2015
TRM003	Czech Republic	Bohemia	Trmice	Grave 10/87	50.637938	13.992275	MCW	MAMS-45794	2329-01-01	-2671	4093	24	human bone	direct	Papac et al. 2021
Sope2	Estonia		Sope	2	59.250537	27.03201	CWC	Poz-10827	2329-01-01	-2671	4093	35	human bone (metatarsus l. dext., female)	direct	Mittnik et al. 2018; Saag et al. 2021; Kriska et al. 2007
TRM006	Czech Republic	Bohemia	Trmice	Grave 109/82	50.637938	13.992275	MCW	MAMS-45796	2305-01-01	-2695	4105	25	human bone	direct	Papac et al. 2021; Buchvaldek et al. 1987; Chochol 1987
Miernow	Poland		Miernow	Barrow 2, feature no. 5	50.3392	20.5839	CWC	KI-5833	2304-01-01	-2696	4105	35	bone	direct	Włodarczak 2001; Włodarczak 2018; Kempisty 1978, 19f.
Ardu2	Estonia		Ardu	2	59.090844	25.35432	CWC	Poz-86648	2297-01-01	-2703	4110	40	human bone (ulna sin., male)	direct	Kriska et al. 2007
PNL002	Czech Republic	Bohemia	Ploníšť nad Labem	Grave 221B	50.250195	15.811275	CW	Poz-9451	2296-01-01	-2704	4110	35	human bone	direct	Papac et al. 2021; Zapotocka 1998; Burgert 2019
Gabulow1	Poland	Lesser Poland	Gabulow 1	1	50.276517	20.571065	CWC	Poz-9451	2296-01-01	-2711	4115	30	charcoal from the grave pit	direct	Jaros & Włodarczak 2007; Gorski & Jarek 2006
KON005	Czech Republic	Bohemia	Konobřez	Grave 26/94	50.555735	13.660563	ECW	MAMS-45789	2269-01-01	-2731	4130	24	human bone	direct	Papac et al. 2021; Dobeš & Buchvaldek 1994
Kruszyn13	Poland		Kruszyn 13	2	52.575015	19.093311	CWC	Poz-33427	2265-01-01	-2735	4140	40	human bone (left talus bone)	direct	Pospieszny et al. 2015
Seligas2	Latvia		Seligas	2	56.325422	24.577742	CWC/Rucewo Culture	Ua-19802	2257-01-01	-2743	4165	60	molar tooth, adult female	direct	Eriksson et al. 2003; Grasis 1996; Grasis 2007
Samborzec23	Poland		Samborzec	Grave 23	50.644631	21.633644	CWC	KI-7931	2255-01-01	-2745	4160	50	human bone	direct	Włodarczak 1999
VIL071	Czech Republic	Bohemia	Vilavěves	Grave 865	50.365945	14.446606	CW	MAMS-45798	2253-01-01	-2747	4171	26	human bone	direct	Papac et al. 2021
KON001	Czech Republic	Bohemia	Konobřez	Grave 10A/91	50.555735	13.660563	ECW	MAMS-45787	2252-01-01	-2748	4167	24	human bone	direct	Papac et al. 2021; Dobeš & Buchvaldek 1993
po81	Poland		Obłackowo	E8-B	52.302047	17.543036	CWC	Poz-36250	2247-01-01	-2753	4160	35	human bone	direct	Pawlak 2013; Malmström et al. 2019
Zernik27	Poland		Zernik 27	Grave 9566A	52.717092	18.27127	CWC	KI-6331	2242-01-01	-2758	4170	40	human bone (femur)	direct	Czebreszuk & Los 1999
STD002	Czech Republic	Bohemia	Vilavěves	Grave 9566A	50.365945	14.446606	CW	MAMS-45801	2230-01-01	-2770	4176	26	human bone	direct	Papac et al. 2021; Dobeš/Imburský 2013
STB002	Czech Republic	Bohemia	Stadice	Grave 29/87	50.619399	13.961205	CW	MAMS-45792	2229-01-01	-2771	4177	25	human bone	direct	Papac et al. 2021; Čurková et al. (1991)
Zablc398	Poland	Masuria	Zablc	398	53.570443	20.478828	CWC	OxA-X-2417-15	2225-01-01	-2775	4187	31	deer antler from antler belt plate	direct	Pospieszny 2015; Manasterski 2009
VIL007	Poland		Lubcz 2, feature 1	1	50.455187	23.637708	CWC	KI-6297	2223-01-01	-2777	4210	60	human bone	direct	Machnik et al. 2009; Machnik 1999, 232; Włodarczak 2018
VIL008	Czech Republic	Bohemia	Vilavěves	Grave 774	50.365945	14.446606	ECW	MAMS-30758	2210-01-01	-2790	4196	21	human bone	direct	Papac et al. 2021
OB0003A	Czech Republic	Bohemia	Vilavěves	Grave 890	50.365945	14.446606	ECW	MAMS-30759	2190-01-01	-2810	4212	21	human bone	direct	Papac et al. 2021
Zvejnieki137	Latvia		Zvejnieki	Grave 166	50.297275	24.494945	ECW	MAMS-30795	2114-01-01	-2886	4259	23	human bone	direct	Papac et al. 2021
PNL001	Czech Republic	Bohemia	Ploníšť nad Labem	137	57.771561	25.233382	CWC	Ua-19811	2107-01-01	-2893	4289	20	human bone	direct	Eriksson et al. 2003; Zagorska 2006; Pospieszny 2015; Meadows 2014/2016
STD003	Czech Republic	Bohemia	Ploníšť nad Labem	Grave LX	50.250195	15.811275	ECW	MAMS-41376	2106-01-01	-2894	4271	25	human bone	direct	Papac et al. 2021; Vokolek 1981; Chochol 1981
Wereszczyna1_1/2	Czech Republic	Bohemia	Stadice	Grave 67/87	50.619399	13.961205	ECW	MAMS-45793	2079-01-01	-2927	4314	25	human bone	direct	Papac et al. 2021; Čurková et al. (1991)
Wereszczyna1_1/2	Poland	Lesser Poland	Wereszczyna 1	Kurgan 1, grave 2	50.461832	23.596627	CWC	KI-6301	2062-01-01	-2938	4305	45	human bone	direct	Machnik et al. 2009; Machnik 1999, 235; Włodarczak 2018; Baginska 1997, 50-2